**Supplementary Information**

# Chemically defined human vascular laminins for biologically relevant culture of hiPSC-derived brain microvascular endothelial cells

Pedram Motallebnejad, Samira M. Azarin

**Supplementary Materials:**

Supplementary Tables S1-S3

Supplementary Figures S1-S9

Description of cell shape analysis procedure

Macro code used for quantifying internalized vesicles

**Table S1. Primary antibodies used for immunocytochemistry.**

| Primary Antibody (Vendor, Clone or Product Number) | Dilution Factor |
|---|---|
| Mouse monoclonal Occludin (Invitrogen, OC-3F10) | 1:200 |
| Mouse monoclonal Claudin-5 (Invitrogen, 4C3C2) | 1:100 |
| Rabbit polyclonal PECAM-1 (Lab Vision, RB10333P) | 1:50 |
| Mouse monoclonal VE-cadherin (Santa Cruz, BV9) | 1:50 |
| Rabbit polyclonal ZO-1 (Invitrogen, 40-2200) | 1:100 |

**Table S2. Secondary antibodies used for immunocytochemistry.**

| Secondary Antibody Conjugate (Vendor) | Dilution Factor |
|---|---|
| Goat anti mouse Alexa Fluor 488 (ThermoFisher) | 1:200 |
| Goat anti mouse Alexa Fluor 594 (ThermoFisher) | 1:200 |
| Goat anti rabbit Alexa Fluor 488 (ThermoFisher) | 1:200 |
| Goat anti rabbit Alexa Fluor 594 (ThermoFisher) | 1:200 |

**Table S3. Primers used for qRT-PCR assays.**

| Gene Name | Unique ID or Forward and Reverse Sequence | Vendor |
|---|---|---|
| *VWF* | qHsaCED0043330 | BioRad |
| *CDH5* | qHsaCID0016288 | BioRad |
| *OCLN* | qHsaCED0038290 | BioRad |
| *TJP1* | qHsaCID0018062 | BioRad |
| *CLDN5* | qHsaCED0047644 | BioRad |
| *ANGPT2* | qHsaCID0017615 | BioRad |
| *MMP2* | qHsaCED0042560 | BioRad |
| *MMP9* | qHsaCID0011597 | BioRad |
| *MMP1* | qHsaCED0048106 | BioRad |
| *LAMA5* | qHsaCED0044330 | BioRad |
| *FN1* | qHsaCED0043611 | BioRad |
| *PECAM1* | Fwd sequence: TGCCGTGGAAAGCAGATACT<br>Rev sequence: TTCCAGGGATGTGCATCTGG | BioRad |
| *GAPDH* | qHsaCED0038674 | BioRad |
| *ANGPT1* | qHsaCED0045626 | BioRad |

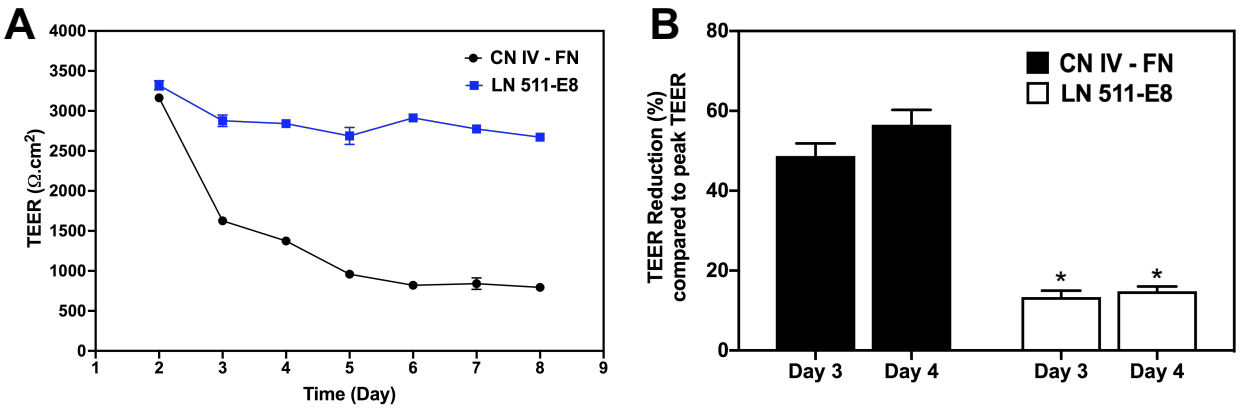


**Figure S1.** TEER measurement results for iBMECs differentiated from the ACS-1024 cell line. (A) TEER values for ACS-1024-derived iBMECs cultured on LN 511-E8 compared to CN IV-FN. (B) TEER reduction compared to peak TEER for ACS-1024-derived iBMECs. * indicates $P < 0.005$ compared to the CN IV-FN condition on the same day.

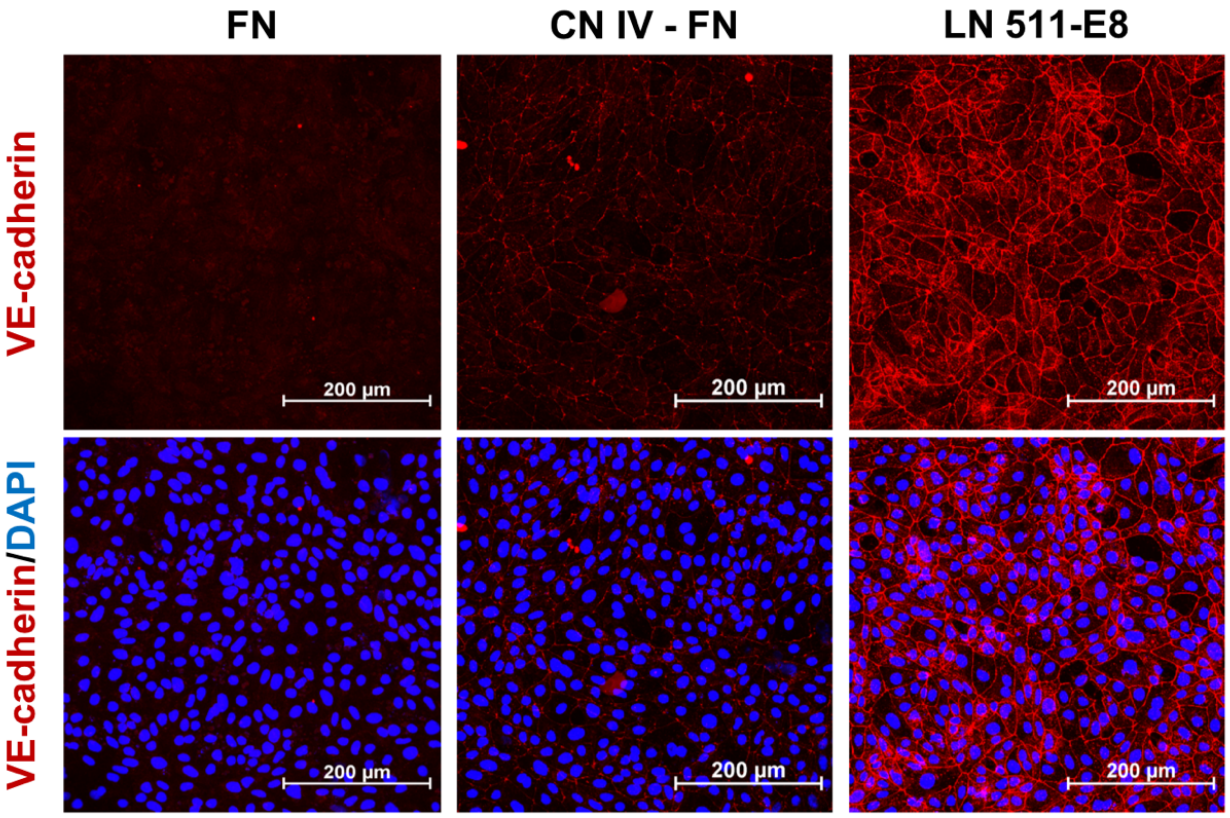


**Figure S2.** The presence of fibronectin decreases junctional expression of VE-cadherin. Imaging was performed 2 days following subculture of iBMECs onto the specified ECM. Top row shows images of VE-cadherin staining and bottom row shows merged images of VE-cadherin and nuclei (stained with DAPI and indicated in blue). Images are maximum intensity projections of confocal z-stacks. Scale bars indicate 200 µm.

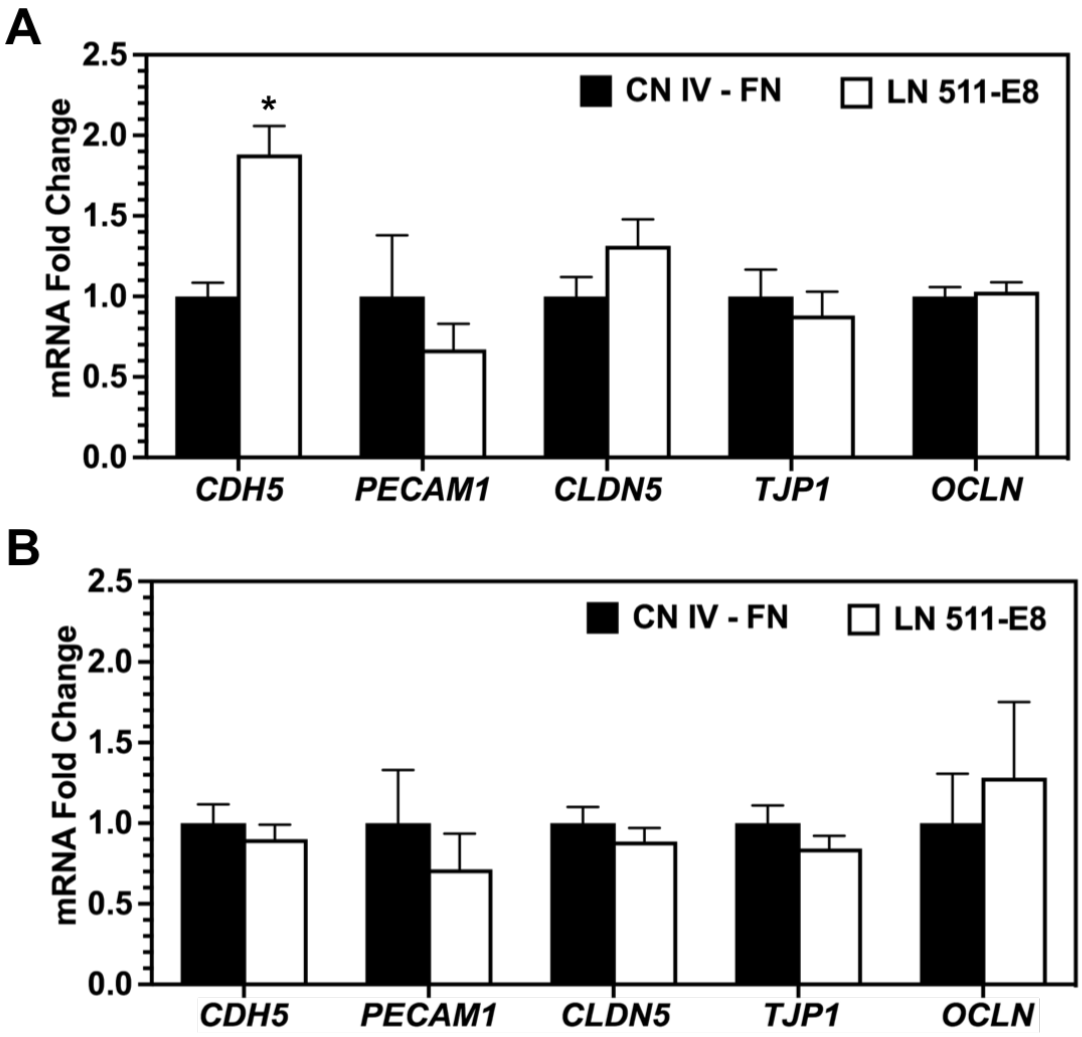


**Figure S3.** Gene expression analysis of tight junction (*CLDN5, TJP1, OCLN*) and adherens junction (*CDH5, PECAM1*) proteins in iBMECs on CN IV-FN or LN 511-E8 4 days after seeding on each ECM. (A) and (B) show the results for two separate biological replicates. Note that VE-cadherin (*CDH5*) expression is upregulated in (A), but unchanged in (B). Fold change is relative to CN IV-FN condition for each gene. * indicates $P < 0.01$ relative to CN IV-FN.

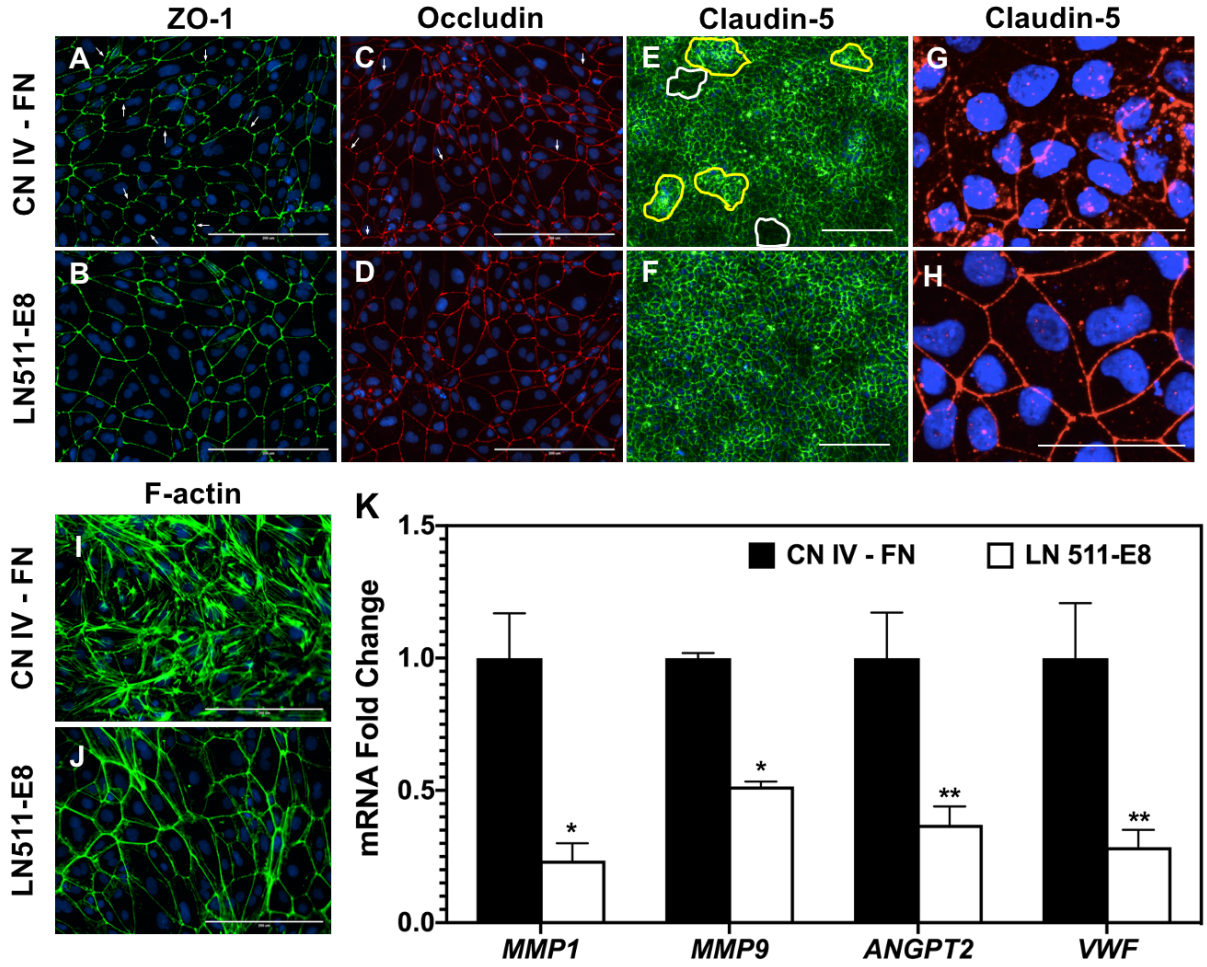


**Figure S4.** Immunocytochemistry and qRT-PCR results for iBMECs differentiated from the ACS-1024 cell line 4 days after subculture on CN IV-FN or LN 511-E8. (A-H) Fluorescence microscopy images of ZO-1 (A,B), occludin (C,D), and claudin-5 (E-H) on CN IV-FN (A,C,E,G) or LN 511-E8 (B,D,F,H). Scale bars indicate 200 µm for (A-F) and 25 µm for (G,H). For claudin-5 images, both low (E,F) and high (G,H) magnification images are provided. The areas outlined in yellow in (F) indicate regions with internalized claudin-5, and areas outlined in white indicate regions with low junctional claudin-5 expression. (G) and (H) show higher magnification images of regions with low claudin-5 expression. For all markers, culture on LN 511-E8 improves junctional expression. (I,J) F-actin immunostaining of iBMECs on CN IV-FN (I) or LN 511-E8 (J). Scale bars indicate 200 µm. Less stress fibers are visible in iBMECs on LN 511-E8. (K) qRT-PCR analysis of *MMP1*, *MMP9*, *ANGPT2*, and *VWF* demonstrates that expression of all four genes is significantly lower on LN 511-E8 than CN IV-FN. Fold change is relative to CN IV-FN condition for each gene. * indicates $P < 0.005$ and ** indicates $P < 0.01$ relative to CN IV-FN.

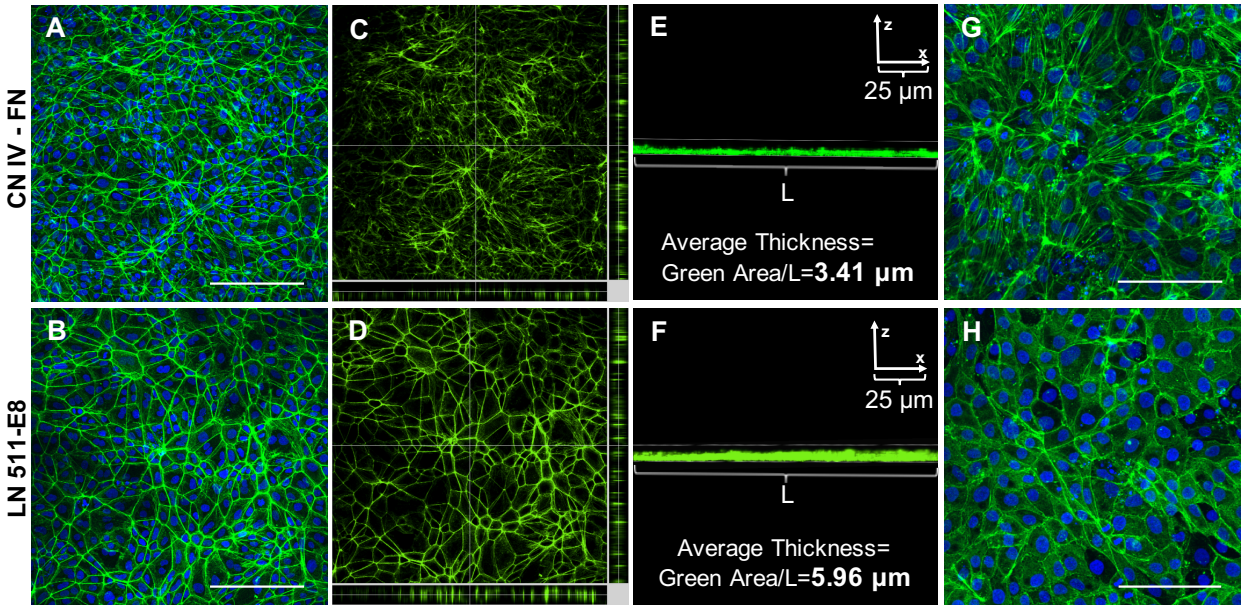


**Figure S5.** F-actin staining of iBMECs on CN IV-FN and LN 511-E8. (A,B) Images of F-actin (green) and nuclei (blue) for iBMECs on CN IV-FN (A) or LN 511-E8 (B) 2 days after subculture. (C,D) Middle plane image of F-actin staining with x and y axis projection of iBMECs on CN IV-FN (C) or LN 511-E8 (D) 2 days after sub-culture. Many stress fibers are visible in the CN IV-FN sample, while F-actin is mostly junctional on LN 511-E8. (E,F) Average height of F-actin expression for the iBMECs on CN IV-FN (E) and LN 511-E8 (F) 2 days after subculture. (G,H) F-actin staining 4 days after subculture on CN IV-FN (G) or LN 511-E8 (H). Nuclei are stained with DAPI and indicated in blue. Images in (A,B,G,H) are maximum intensity projections of confocal z-stacks, and scale bars indicate 100 µm.

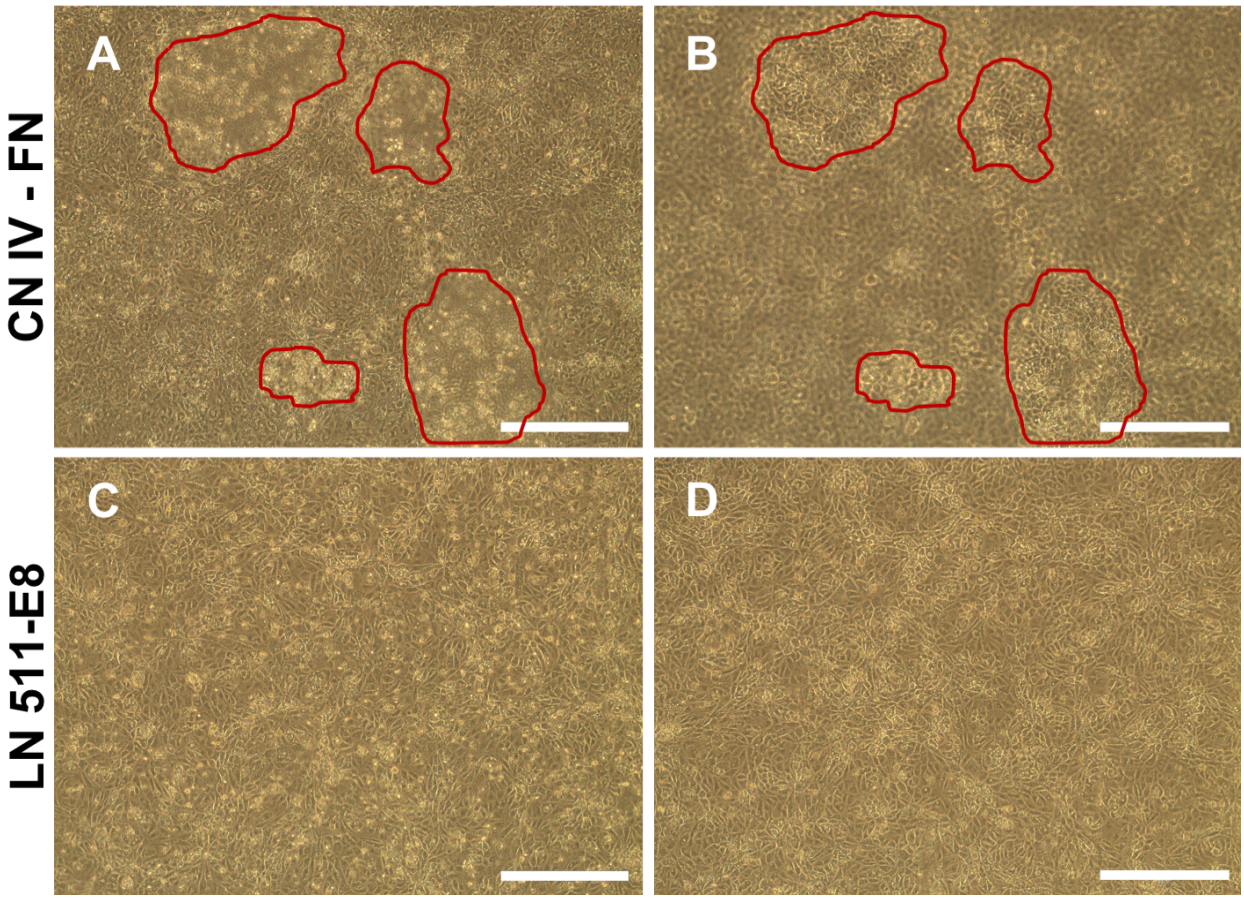


**Figure S6.** Formation of dome-like structures in the iBMEC monolayer on CN IV-FN. (A,B) Images from a lower focal plane (A) and upper focal plane (B) of the same region of iBMECs on CN IV-FN 4 days after subculture. Examples of dome-like structures, in which the cell monolayer is in focus at the higher focal plane, are outlined in red. (C,D) Images of two different regions of the iBMEC monolayer on LN 511-E8, demonstrating the absence of dome-like structures on LN 511-E8. Scale bars indicate 400 μm for all images.

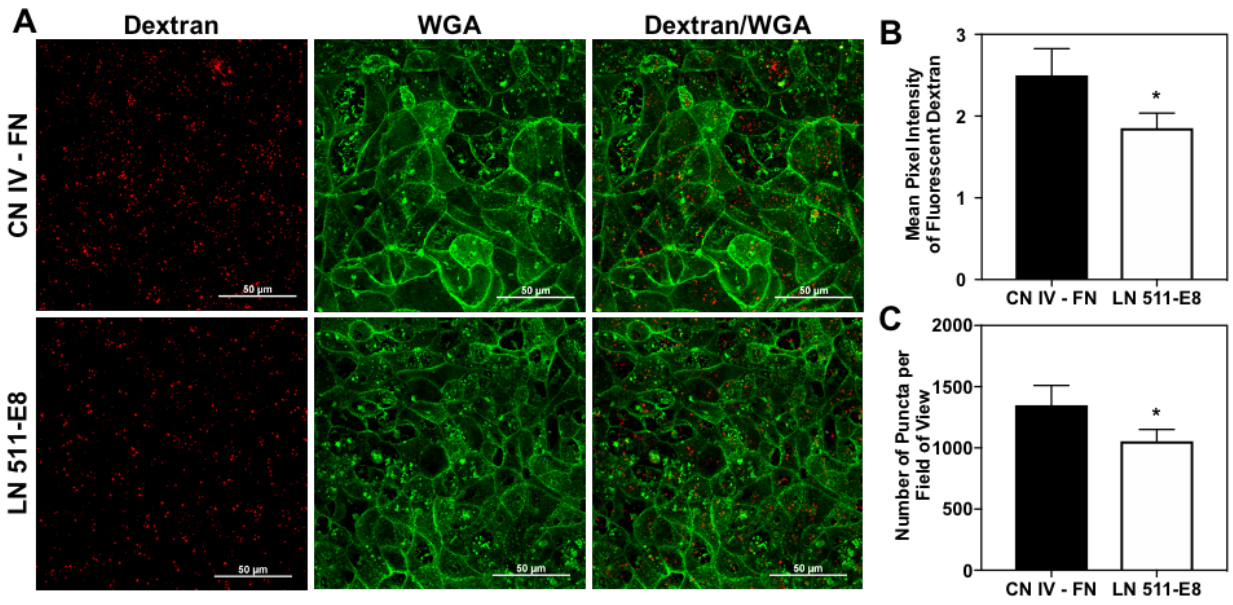


**Figure S7.** Analysis of fluid endocytosis level in iBMECs on LN 511-E8 compared to CN IV-FN. (A) Confocal microscopy images of iBMECs (4 days after subculture) incubated with 1 mg/ml rhodamine B-conjugated dextran, followed by fixation and staining with Oregon Green 488-conjugated WGA. Scale bars indicate 50 µm and images are maximum intensity projections of confocal z-stacks. (B,C) Quantification of mean pixel intensity (B) and the number of fluorescent puncta per image (field of view) (C) in dextran images for iBMECs on CN IV-FN and LN 511-E8. * indicates $P < 0.001$. Results represent 16 analyzed images per condition (2 images per well) from 2 independent rounds of differentiation.

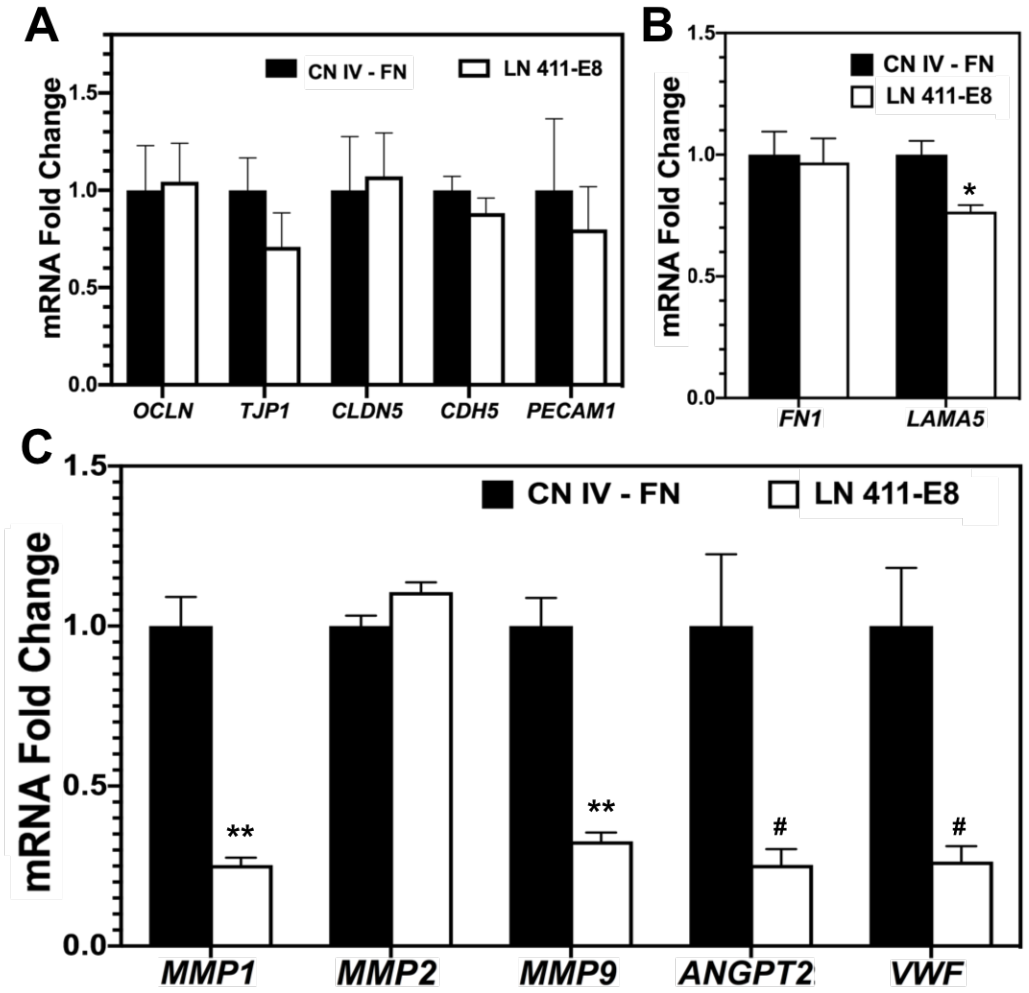


**Figure S8.** Gene expression analysis of iBMECs on LN 411-E8 compared to CN IV-FN. (A-C) Expression of junctional proteins (A), ECM proteins (B), and genes associated with activated endothelium (C) 4 days after subculture on each ECM. Fold change is relative to CN IV-FN condition for each gene. * indicates $P<0.05$, # indicates $P < 0.01$, and ** indicates $P < 0.005$ relative to CN IV-FN.

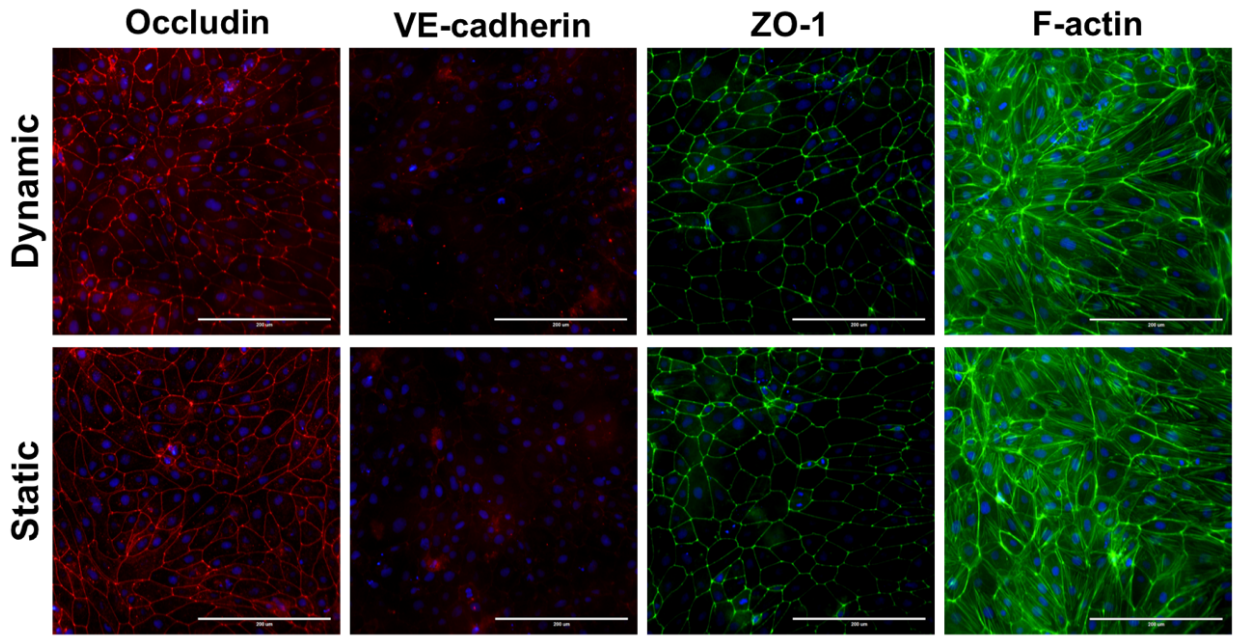


**Figure S9.** Effect of shear stress on junctional protein expression of iBMECs cultured on CN IV-FN. iBMECs were seeded in microfluidic devices and maintained under static conditions for 1 day to reach 100% confluency. Next, for culture under dynamic conditions, devices were connected to a syringe pump and were exposed to 4 dyne/cm$^2$ shear stress for 24 hours before fixation and staining of the iBMECs. Nuclei are stained with DAPI and indicated in blue. Scale bars indicate 200 μm.

**Description of cell shape analysis procedure**

The procedure for cell shape analysis is summarized in the macro code below. This macro can be run in Fiji (ImageJ) in order to obtain the morphological parameters of the cells in a given image. A comment (in bold font) is added to the end of each section of the code to describe the function of that part.

```
makeLine(1248, 910, 808, 910);
run("Set Scale...", "known=200 unit=um");
```
**//sets scale (numbers after makeLine and run functions vary based on the image)**

```
run("8-bit");
```
**//converts the picture to binary**

```
run("Subtract Background...", "rolling=20");
```
**//reduces the noise and background**

```
run("Find Edges");
```
**//highlights the cell boundaries**

```
setAutoThreshold("Huang");
setThreshold(0, 16);
run("Convert to Mask")
```
**//adjusts the threshold and optimizes it for analysis**

```
run("Fill Holes");
```
**//connects the cell boundary lines**

```
run("Analyze Particles...", "size=200-Infinity circularity=0.10-1.00 show=Outlines display exclude summarize in_situ");
```
**//applies the shape analysis command and excludes any recognized particle with surface area smaller than 200 $\mu m^2$ and circularity smaller than 0.1 to eliminate outliers**

**Macro code used for quantifying internalized vesicles**

The “Analyze Particle” command was used to quantify the number of vesicles per image with the macro code shown below. The number of identified particles using this code was recorded to generate the data.

```
run("8-bit");
setAutoThreshold("Default dark");
setThreshold(20, 255);
setOption("BlackBackground", false);
run("Convert to Mask");
run("Analyze Particles...", "size=2-Infinity display clear include summarize in_situ");
```